Impact of Porosity and Boundary Scattering on Thermal Transport in Diameter Modulated Nanowires

Abhinav Malhotra[†,1], Gozde Tutuncuoglu[†,1,2], Sampath Kommandur[†,3], Patrick Creamer[3], Aravindh Rajan[3], Amar Mohabir[1], Shannon Yee[3], Michael A. Filler*[,1], Martin Maldovan*[1,4]

1. School of Chemical & Biomolecular Engineering, Georgia Institute of Technology, Atlanta, GA, 30332, USA.
2. Currently at Electrical and Computer Engineering Department, Wayne State University, Detroit, MI, 48202, USA
3. G.W.W. School of Mechanical Engineering, Georgia Institute of Technology, Atlanta, GA, 30332, USA
4. School of Physics, Georgia Institute of Technology, Atlanta, GA, 30332, USA

† *A.M, G.T, and S.K contributed equally to this paper.*
* *Corresponding authors, email: maldovan@gatech.edu (M.M), michael.filler@chbe.gatech.edu (M.A.F.)*

Keywords: thermal transport, modulated silicon nanowires, porosity, phonon boundary scattering, nanoscale conduction

ABSTRACT

We study the thermal conductivity of diameter modulated Si nanowires to understand the impact of different nanoscale transport mechanisms as a function of nanowire morphology. Our investigation couples transient suspended microbridge measurements of diameter modulated Si nanowires synthesized via vapor-liquid-solid growth and dopant selective etching with predictive Boltzmann transport modeling. We show that the presence of a low thermal conductivity phase (i.e., porosity) dominates the reduction in effective thermal conductivity, and is supplemented by increased phonon-boundary scattering. The relative contributions of both mechanisms depend on the details of the nanoscale morphology. Our findings provide valuable insight into the factors that govern thermal conduction in complex nanoscale materials.

INTRODUCTION

A comprehensive understanding of the contributions of different thermal transport mechanisms in materials with complex nanoscale morphologies, especially those with composite and periodic structures, remains elusive and complicates *a priori* materials design. Such processes are often interrogated using Si nanostructures, such as nanowires[1–7] and nanomeshes,[8–11] because currently available fabrication methods allow for a rich and tunable palette of morphologies. The situation is well understood for relatively simple nanostructures, such as Si nanowires where phonon-boundary scattering dominates thermal transport.[12,13] The diffusive scattering of phonons at surfaces shortens their mean free paths (MFPs), and the thermal conductivity of the nanostructure is reduced with respect to bulk.[6,14] Morphologically, thermal conductivity can be tailored via control of diameter[3,4,6] and surface roughness.[1,5,15] Investigations of modulated nanostructures (such as 'corrugated' nanowires[16–18] and nanoslot films[19]) have also indicated the dominance of phonon-boundary scattering. For structures such as Si nanomeshes,[8,10,20,21] the impact of replacing solid material by a fluid (or another material) must be considered at the same time as phonon-boundary scattering. Material replacement is an effective route to engineer thermal conductivity of both nanoscale and macroscale systems. For instance, extremely low thermal conductivity arises in nano-porous silicon[22] and the thermal insulating properties of aerogels stem from their substantial porosity.[23] In the presence of simultaneously periodic and smooth interfaces at the nanoscale, coherent interference may also be active.[20,21] Additional transport mechanisms, including 'phonon-backscattering,'[24] 'phonon-trapping,'[25] and 'Sharvin resistance,'[26] have been proposed in studies of periodic 'fishbone' and 'scallop' shaped nanowires.[24–26] The number of proposed mechanisms, many of which apply to the specifics and/or conditions of the nanostructure under investigation, indicates that additional

studies are needed to fully understand phonon transport in complex nanostructures and quantify the impact of different mechanisms underlying thermal conduction.

Here, we study diameter-modulated Si nanowires to better understand the governing thermal transport mechanisms in periodic and composite nanostructures. Our methodology combines: (i) bottom-up vapor-liquid-solid (VLS) growth and dopant selective etching[27] to program the morphology of Si nanowires, (ii) a transient suspended four-microbridge thermal conductivity measurement that accounts for thermal contact resistance, and (iii) predictive Boltzmann-transport modeling to predict the thermal conductivity. Our results and analysis show that etching induced material removal and increased diffusive phonon-boundary scattering both play a role in the reduction of thermal transport in diameter-modulated Si nanowires. The relative contribution of each mechanism depends on the details of nanoscale morphology. These insights will be useful for the design of future thermoelectric, electronic, optoelectronic, and photovoltaic devices.[28–32]

EXPERIMENTS

Periodically modulated Si nanowires, as schematically illustrated in Figure 1a, are synthesized by a combination of dopant modulation during VLS growth and post-growth dopant selective KOH etching.[27] A total of seven (n = 7) modulated nanowires with mean unetched diameter of 172.8 nm (standard deviation 5.5 nm) are fabricated. Temperature dependent thermal conductivity measurements are then performed on single nanowires with a modified suspended four microbridge electro-thermal measurement technique developed by Kim *et al*.,[33] which accounts for thermal contact resistance at the nanowire and the bridge interface. To predict thermal transport, we develop a phonon transport model that considers the frequency and temperature dependence of phonon transport in Si.[14,34] The two sections (i.e. etched and unetched

sections) of the modulated nanowire are modeled using this phonon transport model, and their average is used to determine the thermal conductivity of the material κ_{mat}. By using the material thermal conductivity κ_{mat}, effective medium theory formulation is applied to obtain the effective thermal conductivity κ_{eff} of the modulated nanowire This effective medium theory is also validated against finite-element based COMSOL simulations. To compare the κ_{eff} predictions with experiments, the experimentally measured thermal conductance G is converted to effective thermal conductivity using $\kappa_{eff} = GL/A$, where L is the length of the nanowire between microbridges, and A is the unetched nanowire cross-sectional area. Methods for sample preparation, thermal conductivity measurements, and analytical modeling are fully detailed in the Supporting Information (SI).

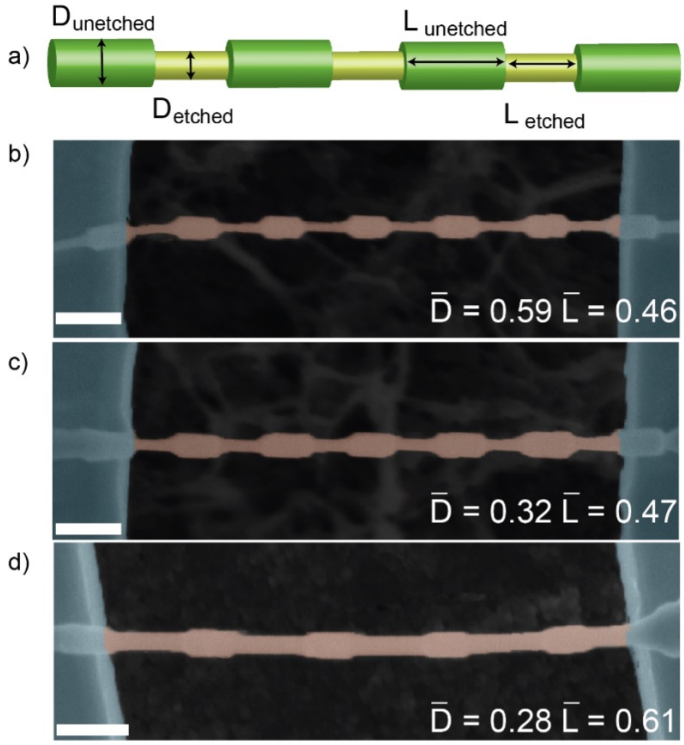

Figure 1. (a) Sketch of a diameter modulated Si nanowire demonstrating the etched and unetched length and diameter; (b)-(d) SEM images of diameter modulated Si nanowires with different $\bar{D}$ and $\bar{L}$ values measured with the transient suspended microbridge technique. Scale bars, 500 nm. The images are false colored for clarity with red highlighting the nanowire and blue highlighting the Pt coated SiN_x microbridges.

We define two dimensionless parameters, $\overline{D}$ and $\overline{L}$, to quantify the magnitude and periodicity of the diameter modulation, respectively. $\overline{D}$ is defined as:

$$\overline{D} = {(D_{unetched} - D_{etched})}/{D_{unetched}} = {\Delta D}/{D_{unetched}} \quad (1)$$

where D_{etched} is the diameter of the nominally undoped segments following dopant selective etching, and $D_{unetched}$ is the diameter of the doped segments, which is equivalent to the original nanowire diameter as these segments do not etch appreciably. $\overline{D}$ varies from 0 for nanowires without selective etching to 1 for nanowires where segments are entirely etched. Similarly, $\overline{L}$ is defined as:

$$\overline{L} = {L_{etched}}/{(L_{unetched} + L_{etched})} \quad (2)$$

where L_{etched} is the length of the etched (*i.e.*, nominally undoped) segments and $L_{unetched}$ is the length of the unetched (*i.e.*, doped) segments. $\overline{L}$ ranges from 0 for nanowires that do not etch appreciably (*i.e.,* fully doped) to 1 when the entire nanowire etches (*i.e.*, no intentional doping). Thus, nanowires with large values of $\overline{D}$ and $\overline{L}$ exhibit a greater amount of material removal. Figures 1b-d show a selection of periodically modulated Si nanowires with different $\overline{D}$ and $\overline{L}$ values.

RESULTS

Figure 2 compares representative temperature dependent effective thermal conductivity κ_{eff} measurements and thermal transport calculations of undoped, dopant modulated, and dopant and diameter modulated Si nanowires between 50 K and room temperature. The measured thermal conductivity κ_{eff} of all nanowires is lower than that of bulk Si, as expected from diffuse phonon-boundary scattering.[35] A boundary-scattering dominant low temperature region and phonon-

phonon/impurity scattering dominant high temperature region is observed for all samples. For unetched nanowires, either nominally undoped (Figure 2a) or dopant modulated (Figure 2b), the measured and predicted thermal conductivities κ_{eff} are in agreement across the entire temperature range. A small reduction (from ~55 to 50 W/m-K at 125 K) in κ_{eff} is seen upon

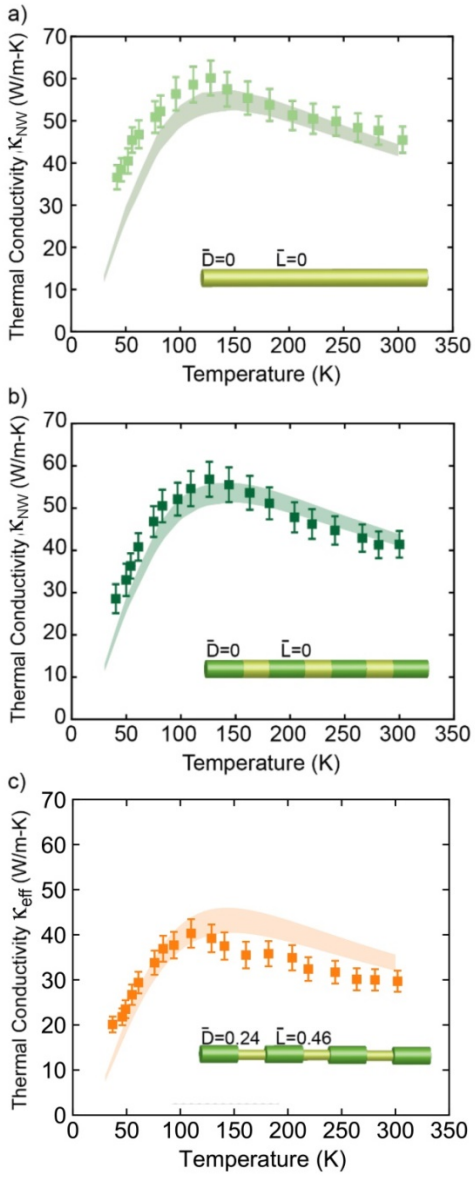

Figure 2. Temperature dependent effective thermal conductivity measurements and predictions for (a) a nominally undoped Si nanowire ($D_{unetched}$ = 159 nm), (b) a dopant modulated Si nanowire ($D_{unetched}$ = 154 nm), and (c) a dopant and diameter modulated Si nanowire. The nanowires measured in (b) and (c) are from the same growth run. All prediction bands account for a ±10 nm uncertainty in diameters, and all measurement uncertainties are calculated using a Monte Carlo approach described in SI.[36,37]

doping (Figure 2a vs. Figure 2b). This is consistent with additional phonon point-defect scattering since the weak electron-phonon interactions in Si is demonstrated in previous studies.[38] Measurements of nanowires with diameter modulation show a further reduction of κ_{eff} (Figure 2b vs. Figure 2c). Considering the independent development of theoretical predictions and experimental measurements, uncertainty in low temperature phonon MFPs, and experimental surface characterization, the agreement between theory and experiments is reasonable. Despite the differences, experiments and theoretical predictions clearly show how the introduction of diameter modulation by etching leads to a considerable reduction in thermal transport in the nanostructure.

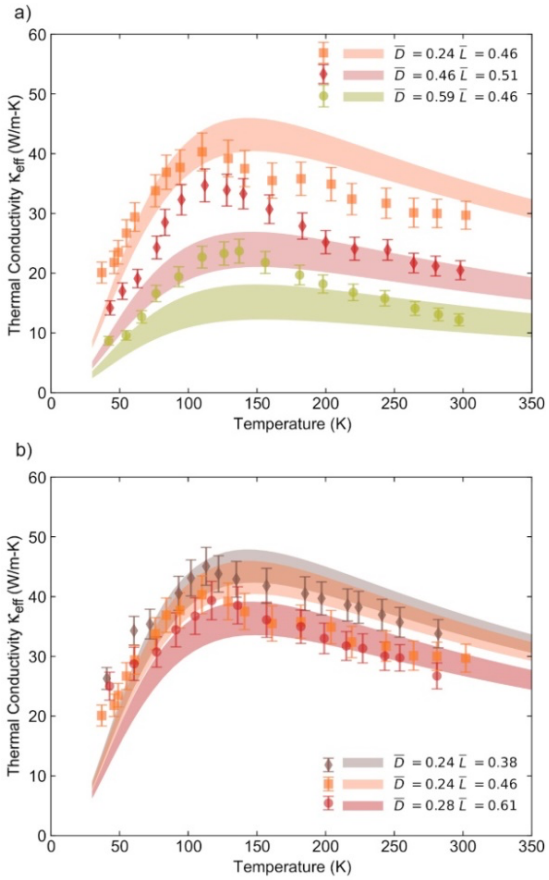

Figure 3. Temperature dependent effective thermal conductivity measurements and predictions of diameter modulated Si nanowires with varying (a) $\overline{D}$ and (b) $\overline{L}$. All prediction bands account for a ±10 nm uncertainty in diameters, and all measurement uncertainties are calculated using a Monte Carlo approach detailed in SI.

We now study the impact of $\bar{D}$ and $\bar{L}$ on the observed reduction of effective thermal conductivity. Figure 3 shows the measured and predicted effective thermal conductivity of diameter modulated nanowires between 50 K and room temperature possessing similar $D_{unetched}$ (mean 172.8 nm, relative standard deviation 3.2 %) and $L_{unetched}$ (mean 285.4 nm, relative standard deviation 8.5 %). For nanowires with varying $\bar{D}$ and constant $\bar{L}$ (Figure 3a), both measurement and modeling indicate that thermal conductivity κ_{eff} decreases as $\bar{D}$ increases. In comparison, the impact of $\bar{L}$ on thermal conductivity κ_{eff} for nanowires with a fixed $\bar{D}$ is found to be weaker for all temperatures for the considered range of $\bar{D}$ values (Figure 3b). To examine the role of $\bar{D}$ and $\bar{L}$ more closely, we plot room temperature thermal conductivity κ_{eff} for modulated nanowires as a function of $\bar{D}$ and $\bar{L}$ in Figure 4a and 4b, respectively. Both measurement and modeling show a strong correlation between $\bar{D}$ and κ_{eff} (Pearson's correlation coefficient, R = -0.948) while a weak correlation is observed between $\bar{L}$ and κ_{eff} (R = -0.05) for the range of structures considered. When these data are replotted as a function of porosity, i.e., the ratio of the volume of the etched material to the volume of the original structure, $\phi = (2 - \bar{D})\bar{D}\bar{L}$ in Figure 4c, it is observed that the thermal conductivity κ_{eff} of diameter modulated nanowires reduces with increasing porosity. Thus, increasing $\bar{D}$ and $\bar{L}$ suppresses thermal conduction as more material is removed. This reduction in nanoscale thermal conductivity is due to both phonon boundary scattering and porosity, which are analyzed next.

We now assess the contributions of material removal (i.e., porosity) and phonon-boundary scattering on the observed reduction in effective thermal conductivity for diameter-modulated Si nanowires. To estimate the contribution of each mechanism, we simulate diameter-modulated nanowires where the thermal conductivity is due to (i) material removal alone (i.e.,

assuming phonon-boundary scattering is the same for etched and unetched segments) or (ii) both material removal and changes to phonon-boundary scattering.

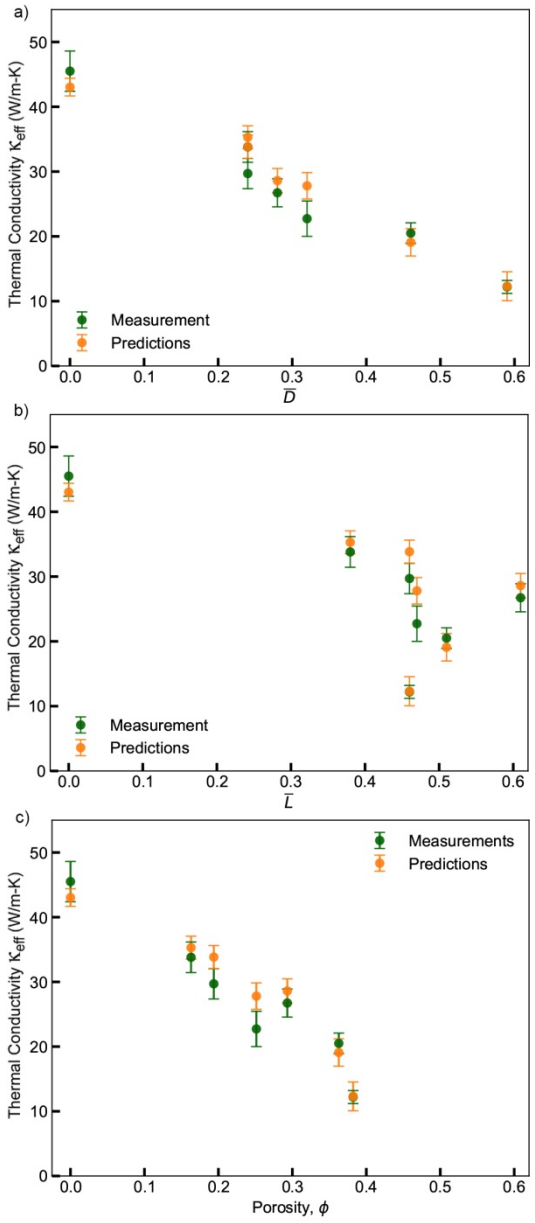

Figure 4. Room-temperature effective thermal conductivity measurements and model predictions plotted as a function of (a) $\overline{D}$, (b) $\overline{L}$, and (c) porosity for all studied nanowires.

Figure 5 shows the predicted thermal conductivities as a function of temperature for the unetched Si nanowire (gray), a diameter modulated Si nanowire where only material removal effects are included (orange), and a diameter modulated Si nanowire including contributions

from both material removal and phonon-boundary scattering (red). We find that replacing solid material with a low conducting air/vacuum phase causes the majority of the reduction of thermal conductivity κ_{eff}; however, both contributions are important. For the nanowire in Figure 5a (smaller $\overline{D}$ and $\overline{L}$) at 300 K, material removal reduces the thermal conductivity by ~22% from the unetched nanowire and the addition of phonon-boundary scattering further reduces thermal conductivity by ~12%. In contrast, for the nanowire in Figure 5b (larger $\overline{D}$ and $\overline{L}$) at 300 K, material removal caused a significantly higher ~70% reduction whereas phonon-boundary scattering led to a further ~21% reduction.

We note that two thermal conductivities have been considered in the literature: (i) the *effective* thermal conductivity κ_{eff} which includes contributions from both material removal and phonon-boundary scattering (as reported above), and (ii) the *solid material's* intrinsic thermal conductivity κ_{mat}, which is derived from experimental data accounting only for additional phonon-boundary scattering (i.e., neglecting material removal effects, see SI for method). The solid material thermal conductivity κ_{mat} for our modulated nanowires is shown in Figure 6a as a function of etched diameter at room temperature. Red solid symbols show these κ_{mat} values while red solid line shows the theoretical predictions. The material thermal conductivity κ_{mat} ranges from 35-45 W/m-K showing a reduction from Si bulk value κ~150 W/m-K arising due to phonon boundary scattering. The κ_{mat} values for fishbone nanowires,[25] nanoladders,[39] and corrugated nanowires,[18] which, unlike our modulated nanowires, are all planar top-down etched structures, are also included as symbols (squares). For comparison, we consider nanostructures with similar characteristic sizes to our modulated nanowires, i.e. ~100nm and find good agreement across all the nanostructures. In addition, we next compare our results to those reported for nanomeshes[9]. We plot both thermal conductivity values κ_{eff} and κ_{mat} for our

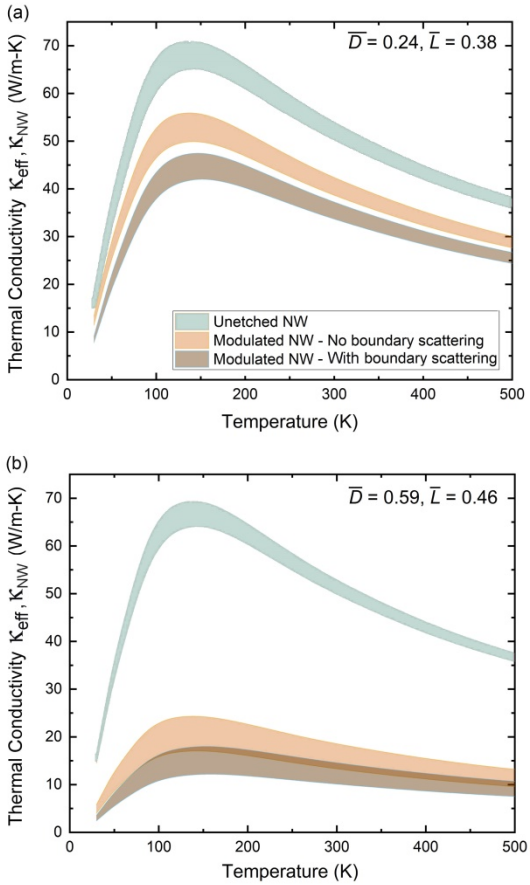

Figure 5. Predicted thermal conductivity values for diameter modulated Si nanowires from this work as a function of temperature: (a) $\overline{D}$ = 0.24 and $\overline{L}$ = 0.38, (b) $\overline{D}$ = 0.59 and $\overline{L}$ = 0.46. Effective thermal conductivity accounting for both material removal and added phonon-boundary scattering is shown in brown, whereas thermal conductivity accounting only for material removal is shown in orange. For comparison, the thermal conductivity of an unetched nanowire is shown in gray on both plots with bands accounting for a ±10 nm diameter uncertainty.

nanowires (with constant $\overline{D}$) along with the data from nanomeshes[9] for a constant neck size (similar to our $\overline{D}$) as a function of $\overline{L}$ in Figure 6b. For the effective thermal conductivity κ_{eff}, we observe a slight reduction as $\overline{L}$ is increased for both our nanowires and literature reported nanomeshes, consistent with the physical interpretation of additional scattering and material removal effects explained above. However, in the case of our nanowires, the solid material thermal conductivity κ_{mat}, shows a near independence with increasing $\overline{L}$, indicating the weak role

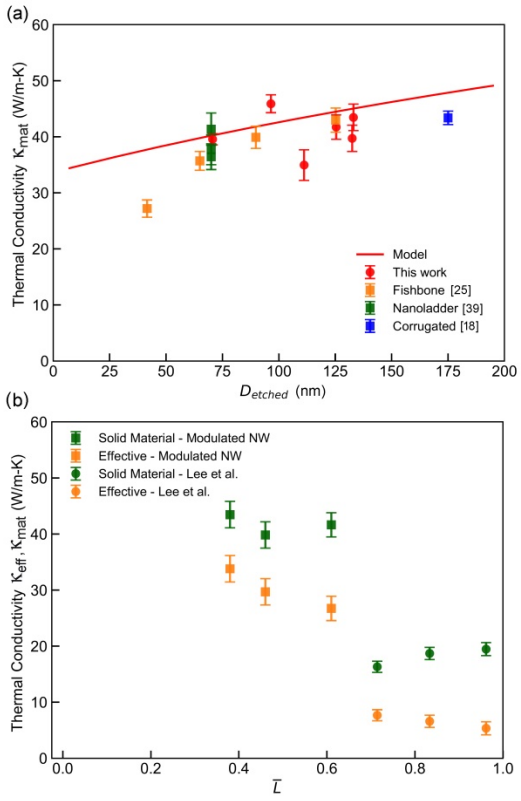

Figure 6. (a) Solid material κ_{mat} at room temperature as a function of D_{etched} (or neck) for our modulated nanowires (circles) and structures from literature (squares). (b) Effective κ_{eff} (orange) and solid material κ_{mat} (green) thermal conductivity plotted as a function of length ratio $\bar{L}$ for modulated nanowires with constant diameter ratio $\bar{D}$ (square) and for nanomeshes from literature (circle).[9]

of scattering from perpendicular walls in impacting intrinsic thermal transport properties. In contrast, in nanomeshes the solid material thermal conductivity κ_{mat} increases with increasing $\bar{L}$. We note that the changes in this material thermal conductivity κ_{mat} in nanomeshes could be explained without invoking the concept of backscattering by considering the diffusive scattering of phonons in the cross-plane direction (i.e., transport where nanostructure boundaries are perpendicular to temperature gradient) where thermal transport is suppressed as compared to the in-plane direction,[40] explaining why removing the contribution from perpendicular walls by making $\bar{L} \sim 1$ with constant $\bar{D}$ can slightly increase material thermal conductivity.

Our data also indicate that coherent effects, such as phonon trapping,[41] are not active in our system. In the presence of coherent interference, a change in structural periodicity (i.e., $\bar{L}$) can modify the phononic density of states, especially at lower temperatures where phonon-phonon interactions are suppressed.[21] However, coherence is most expected when nanostructure dimensions are small (< 20 nm for Si)[42,43] and/or when surfaces are smooth[21] while our current nanowire dimensions are relatively large (~ 100 nm) and post-growth etching increases surface roughness (etched Si surfaces are often rough,[15] in excess of 5 nm in some instances[24]). Careful surface tuning along with tailoring the phonon spectra with alloying and cooling[19] may elicit coherent effects in Si nanostructures.

CONCLUSION

In summary, we combine advances in bottom-up VLS growth and dopant selective etching, detailed predictive thermal conductivity calculations, and transient suspended four microbridge technique to probe and understand phonon transport in diameter modulated Si nanowires. We assess the relative impact of porosity and phonon-boundary scattering on the observed reduction of effective thermal conductivity. While increased porosity is the dominant effect, its relative influence depends on the details of the nanoscale structure. Our phonon transport model is sufficient to capture the phonon dynamics in diameter-modulated Si nanowires enabling accurate predictions of thermal conductivity without invoking alternative mechanisms.

SUPPORTING INFORMATION

Methodological details including nanowire growth, thermal conductivity measurements, error estimation, modeling, and reporting of thermal conductivity in unetched and modulated nanowires.

ACKNOWLEDGMENTS

We would like to acknowledge Melanie Brunet Torres for fabricating the measurement devices, Eric Woods for assistance with the focused ion beam, and Juan M. Restrepo-Florez for discussions on effective medium theory. M.A.F. thanks the National Science Foundation for their financial support (CBET-1510934, CBET-1916953). This work was performed in part at the Georgia Tech Institute for Electronics and Nanotechnology, a member of the National Nanotechnology Coordinated Infrastructure (NNCI), which is supported by the National Science Foundation (Grant ECCS-2025462).

REFERENCES

(1) Hochbaum, A. I.; Chen, R.; Delgado, R. D.; Liang, W.; Garnett, E. C.; Najarian, M.; Majumdar, A.; Yang, P. Enhanced Thermoelectric Performance of Rough Silicon Nanowires. *Nature* **2008**, *451* (7175), 163–167. https://doi.org/10.1038/nature06381.

(2) Shi, L.; Li, D.; Yu, C.; Jang, W.; Kim, D.; Yao, Z.; Kim, P.; Majumdar, A. Measuring Thermal and Thermoelectric Properties of One-Dimensional Nanostructures Using a Microfabricated Device. *Journal of Heat Transfer* **2003**, *125* (5), 881. https://doi.org/10.1115/1.1597619.

(3) Li, D.; Wu, Y.; Kim, P.; Shi, L.; Yang, P.; Majumdar, A. Thermal Conductivity of Individual Silicon Nanowires. *Applied Physics Letters* **2003**, *83* (14), 2934–2936. https://doi.org/10.1063/1.1616981.

(4) Walkauskas, S. G.; Broido, D. A.; Kempa, K.; Reinecke, T. L. Lattice Thermal Conductivity of Wires. *Journal of Applied Physics* **1999**, *85* (5), 2579–2582. https://doi.org/10.1063/1.369576.

(5) Feser, J. P.; Sadhu, J. S.; Azeredo, B. P.; Hsu, K. H.; Ma, J.; Kim, J.; Seong, M.; Fang, N. X.; Li, X.; Ferreira, P. M.; Sinha, S.; Cahill, D. G. Thermal Conductivity of Silicon Nanowire Arrays with Controlled Roughness. *Journal of Applied Physics* **2012**, *112* (11), 114306. https://doi.org/10.1063/1.4767456.

(6) Mingo, N.; Yang, L.; Li, D.; Majumdar, A. Predicting the Thermal Conductivity of Si and Ge Nanowires. *Nano Letters* **2003**, *3* (12), 1713–1716. https://doi.org/10.1021/nl034721i.

(7) Mukherjee, S.; Givan, U.; Senz, S.; Bergeron, A.; Francoeur, S.; de la Mata, M.; Arbiol, J.; Sekiguchi, T.; Itoh, K. M.; Isheim, D.; Seidman, D. N.; Moutanabbir, O. Phonon Engineering in Isotopically Disordered Silicon Nanowires. *Nano Lett.* **2015**, *15* (6), 3885–3893. https://doi.org/10.1021/acs.nanolett.5b00708.

(8) Jain, A.; Yu, Y.-J.; Mcgaughey, A. J. H. Phonon Transport in Periodic Silicon Nanoporous Films with Feature Sizes Greater than 100 Nm. *PHYSICAL REVIEW B* **2013**, *87*, 195301. https://doi.org/10.1103/PhysRevB.87.195301.

(9) Lee, J.; Lee, W.; Wehmeyer, G.; Dhuey, S.; Olynick, D. L.; Cabrini, S.; Dames, C.; Urban, J. J.; Yang, P. Investigation of Phonon Coherence and Backscattering Using Silicon Nanomeshes. *Nature Communications* **2017**, *8*. https://doi.org/10.1038/ncomms14054.
(10) Maldovan, M. Narrow Low-Frequency Spectrum and Heat Management by Thermocrystals. *Physical Review Letters* **2013**, *110* (2). https://doi.org/10.1103/PhysRevLett.110.025902.
(11) Wagner, M. R.; Graczykowski, B.; Reparaz, J. S.; El Sachat, A.; Sledzinska, M.; Alzina, F.; Sotomayor Torres, C. M. Two-Dimensional Phononic Crystals: Disorder Matters. *Nano Lett.* **2016**, *16* (9), 5661–5668. https://doi.org/10.1021/acs.nanolett.6b02305.
(12) Cahill, D. G.; Braun, P. V.; Chen, G.; Clarke, D. R.; Fan, S.; Goodson, K. E.; Keblinski, P.; King, W. P.; Mahan, G. D.; Majumdar, A.; Maris, H. J.; Phillpot, S. R.; Pop, E.; Shi, L. Nanoscale Thermal Transport. II. 2003-2012. *Applied Physics Reviews*. American Institute of Physics Inc. January 14, 2014, p 011305. https://doi.org/10.1063/1.4832615.
(13) Malhotra, A.; Maldovan, M. Phononic Pathways towards Rational Design of Nanowire Heat Conduction. *Nanotechnology* **2019**. https://doi.org/10.1088/1361-6528/ab261d.
(14) Malhotra, A.; Maldovan, M. Impact of Phonon Surface Scattering on Thermal Energy Distribution of Si and SiGe Nanowires. *Scientific Reports* **2016**, *6*. https://doi.org/10.1038/srep25818.
(15) Lim, J.; Hippalgaonkar, K.; Andrews, S. C.; Majumdar, A.; Yang, P. Quantifying Surface Roughness Effects on Phonon Transport in Silicon Nanowires. *Nano Letters* **2012**, *12* (5), 2475–2482. https://doi.org/10.1021/nl3005868.
(16) Blanc, C.; Rajabpour, A.; Volz, S.; Fournier, T.; Bourgeois, O. Phonon Heat Conduction in Corrugated Silicon Nanowires below the Casimir Limit. *Appl. Phys. Lett.* **2013**, *103* (4), 043109. https://doi.org/10.1063/1.4816590.
(17) Hori, T. Role of Geometry and Surface Roughness in Reducing Phonon Mean Free Path and Lattice Thermal Conductivity of Modulated Nanowires. *International Journal of Heat and Mass Transfer* **2020**, *156*, 119818. https://doi.org/10.1016/j.ijheatmasstransfer.2020.119818.
(18) Anufriev, R.; Gluchko, S.; Volz, S.; Nomura, M. Quasi-Ballistic Heat Conduction Due to Lévy Phonon Flights in Silicon Nanowires. *ACS Nano* **2018**, *12* (12), 11928–11935. https://doi.org/10.1021/acsnano.8b07597.
(19) Hao, Q.; Xiao, Y.; Chen, Q. Determining Phonon Mean Free Path Spectrum by Ballistic Phonon Resistance within a Nanoslot-Patterned Thin Film. *Materials Today Physics* **2019**, *10*, 100126. https://doi.org/10.1016/j.mtphys.2019.100126.
(20) Maldovan, M. Phonon Wave Interference and Thermal Bandgap Materials. *Nature Materials* **2015**, *14* (7), 667–674. https://doi.org/10.1038/nmat4308.
(21) Ravichandran, J.; Yadav, A. K.; Cheaito, R.; Rossen, P. B.; Soukiassian, A.; Suresha, S. J.; Duda, J. C.; Foley, B. M.; Lee, C. H.; Zhu, Y.; Lichtenberger, A. W.; Moore, J. E.; Muller, D. A.; Schlom, D. G.; Hopkins, P. E.; Majumdar, A.; Ramesh, R.; Zurbuchen, M. A. Crossover from Incoherent to Coherent Phonon Scattering in Epitaxial Oxide Superlattices. *Nature Materials* **2014**, *13* (2), 168–172. https://doi.org/10.1038/nmat3826.
(22) Zhao, Y.; Yang, L.; Kong, L.; Nai, M. H.; Liu, D.; Wu, J.; Liu, Y.; Chiam, S. Y.; Chim, W. K.; Lim, C. T.; Li, B.; Thong, J. T. L.; Hippalgaonkar, K. Ultralow Thermal Conductivity of Single-Crystalline Porous Silicon Nanowires. *Advanced Functional Materials* **2017**, *27* (40), 1702824. https://doi.org/10.1002/adfm.201702824.

(23) Soleimani Dorcheh, A.; Abbasi, M. H. Silica Aerogel; Synthesis, Properties and Characterization. *Journal of Materials Processing Technology*. Elsevier April 1, 2008, pp 10–26. https://doi.org/10.1016/j.jmatprotec.2007.10.060.
(24) Lee, S.; Yoo, H.; Won, W.-Y.; Cho, H.; Seo, M.; Kong, B. D.; Meyyappan, M.; Baek, C.-K. Thermal Conductivity Reduction by Scallop Shaped Surface Modulation in Silicon Nanowires. *Applied Physics Letters* **2020**, *116* (20), 203901. https://doi.org/10.1063/5.0006570.
(25) Maire, J.; Anufriev, R.; Hori, T.; Shiomi, J.; Volz, S.; Nomura, M. Thermal Conductivity Reduction in Silicon Fishbone Nanowires. *Scientific Reports* **2018**, *8* (1). https://doi.org/10.1038/s41598-018-22509-0.
(26) Yang, L.; Zhao, Y.; Zhang, Q.; Yang, J.; Li, D. Thermal Transport through Fishbone Silicon Nanoribbons: Unraveling the Role of Sharvin Resistance. *Nanoscale* **2019**, *11* (17), 8196–8203. https://doi.org/10.1039/c9nr01855g.
(27) Christesen, J. D.; Pinion, C. W.; Hill, D. J.; Kim, S.; Cahoon, J. F. Chemically Engraving Semiconductor Nanowires: Using Three-Dimensional Nanoscale Morphology to Encode Functionality from the Bottom Up. *Journal of Physical Chemistry Letters* **2016**, *7* (4), 685–692. https://doi.org/10.1021/acs.jpclett.5b02444.
(28) Maldovan, M. Sound and Heat Revolutions in Phononics. *Nature*. 2013, pp 209–217. https://doi.org/10.1038/nature12608.
(29) Tervo, E. J.; Gustafson, M. E.; Zhang, Z. M.; Cola, B. A.; Filler, M. A. Photonic Thermal Conduction by Infrared Plasmonic Resonators in Semiconductor Nanowires. *Applied Physics Letters* **2019**, *114* (16), 163104. https://doi.org/10.1063/1.5093309.
(30) Pop, E. Energy Dissipation and Transport in Nanoscale Devices. *Nano Res* **2010**, *3*, 147–169. https://doi.org/10.1007/s12274-010-1019-z.
(31) He, J.; Tritt, T. M. Advances in Thermoelectric Materials Research: Looking Back and Moving Forward. *Science*. American Association for the Advancement of Science September 29, 2017. https://doi.org/10.1126/science.aak9997.
(32) Malhotra, A.; Kothari, K.; Maldovan, M. Cross-Plane Thermal Conduction in Superlattices: Impact of Multiple Length Scales on Phonon Transport. *Journal of Applied Physics* **2019**, *125* (4), 044304. https://doi.org/10.1063/1.5065904.
(33) Kim, J.; Ou, E.; Sellan, D. P.; Shi, L. A Four-Probe Thermal Transport Measurement Method for Nanostructures. *Review of Scientific Instruments* **2015**, *86* (4), 044901. https://doi.org/10.1063/1.4916547.
(34) Maldovan, M. Thermal Conductivity of Semiconductor Nanowires from Micro to Nano Length Scales. *Journal of Applied Physics* **2012**, *111* (2). https://doi.org/10.1063/1.3677973.
(35) Glassbrenner, C. J.; Slack, G. A. Thermal Conductivity of Silicon and Germanium from 3°K to the Melting Point. *Physical Review* **1964**, *134* (4A). https://doi.org/10.1103/PhysRev.134.A1058.
(36) Bougher, T. L.; Yates, L.; Lo, C. F.; Johnson, W.; Graham, S.; Cola, B. A. Thermal Boundary Resistance in GaN Films Measured by Time Domain Thermoreflectance with Robust Monte Carlo Uncertainty Estimation. *Nanoscale and Microscale Thermophysical Engineering* **2016**, *20* (1), 22–32. https://doi.org/10.1080/15567265.2016.1154630.
(37) Papadopoulos, C. E.; Yeung, H. Uncertainty Estimation and Monte Carlo Simulation Method. *Flow Measurement and Instrumentation* **2001**, *12* (4), 291–298. https://doi.org/10.1016/S0955-5986(01)00015-2.

(38) Liao, B.; Qiu, B.; Zhou, J.; Huberman, S.; Esfarjani, K.; Chen, G. Significant Reduction of Lattice Thermal Conductivity by the Electron-Phonon Interaction in Silicon with High Carrier Concentrations: A First-Principles Study. *Physical Review Letters* **2015**, *114* (11). https://doi.org/10.1103/PhysRevLett.114.115901.
(39) Park, W.; Sohn, J.; Romano, G.; Kodama, T.; Sood, A.; Katz, J. S.; Kim, B. S. Y.; So, H.; Ahn, E. C.; Asheghi, M.; Kolpak, A. M.; Goodson, K. E. Impact of Thermally Dead Volume on Phonon Conduction along Silicon Nanoladders. *Nanoscale* **2018**, *10* (23), 11117–11122. https://doi.org/10/gdn2jx.
(40) Maldovan, M. Specular Reflection Leads to Maximum Reduction in Cross-Plane Thermal Conductivity. *Journal of Applied Physics* **2019**, *125* (22), 224301. https://doi.org/10.1063/1.5092341.
(41) Nika, D. L.; Cocemasov, A. I.; Isacova, C. I.; Balandin, A. A.; Fomin, V. M.; Schmidt, O. G. Suppression of Phonon Heat Conduction in Cross-Section-Modulated Nanowires. *Physical Review B - Condensed Matter and Materials Physics* **2012**, *85* (20). https://doi.org/10.1103/PhysRevB.85.205439.
(42) Honarvar, H.; Yang, L.; Hussein, M. I. Thermal Transport Size Effects in Silicon Membranes Featuring Nanopillars as Local Resonators. *Applied Physics Letters* **2016**, *108* (26), 263101. https://doi.org/10.1063/1.4954739.
(43) Wingert, M. C.; Chen, Z. C. Y.; Dechaumphai, E.; Moon, J.; Kim, J. H.; Xiang, J.; Chen, R. Thermal Conductivity of Ge and Ge-Si Core-Shell Nanowires in the Phonon Confinement Regime. *Nano Letters* **2011**, *11* (12), 5507–5513. https://doi.org/10.1021/nl203356h.

TOC GRAPHIC